Application of unconditioned nanostructured thermoplastic based strain gauge sensor in wearable electronics

Francesco Maita, Veronica Piccialli, Flavia Pensa, Marco Scatto, Massimiliano Ruggeri and Luca Maiolo

***Abstract*— Wearable electronics is now revolutionizing the world of smart sensors offering tremendous solutions to a variety of applications that span from biomedical market to gaming and fashion sectors. In this scenario, physical sensors play a crucial role since they offer a fast and reliable feedback of the human motion, even for fine gesture, and can detect vital physiological parameters such as breathing and heart beating, while being able to be easily integrated on textile. Among wearable physical sensors, thermoplastic materials are utilized for their sensitivity and high stretchability. Moreover, these materials exhibit a good chemical resistance and implement low cost manufacturing processes. In this work, we report a full characterization of a new thermoplastic nanocomposite material comparing its performances with and without pre-conditioning for strain up to 20%. Together with a measured gauge factor of about 10, sensors without pre-conditioning exhibits very good stability and they result to be a good candidate for wearable applications. We demonstrate this statement analyzing the performance of a smart wristband prototype that integrates these strain gauges, obtaining very high performance of the sensors without pre-strain in gesture recognition tasks with an accuracy and F-score of about 94%.**

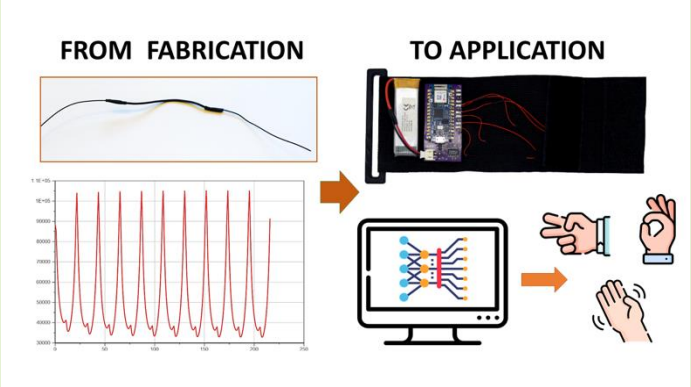

***Index Terms*—Smart wristband, strain gauge, thermoplastic nanocomposite, wearable electronics**

I. Introduction

The world of sensors is becoming more and more mature, offering multiple solutions that can be deployed pervasively on urban infrastructures or on a person's garment and devices. This trend must match the customer preferences to become captivating and diffuse into the market. In this sense, a winning sensing technology should be generally transparent to the final user. This means that device integration and miniaturization is the key to manufacture products with a successful feedback from the market. Indeed, consumers are now accustomed to obtain complex information from their devices and they demand for multipurpose sensing platforms that can easily merge data and process novel information quickly.

Wearable electronics can represent a valuable technology to collect multiple sensing parameters, manage these signals (e.g. filter, amplify and digitalize data) and transfer significant information through cloud computing [1-3]. Wearable electronics has been conceived as intrinsically autonomous system that can harvest energy by external sources (e.g. solar cells or human motion) or can even show self-healing properties, guaranteeing long device lifetime and reducing the environmental impact [4-7]. Many different classes of sensors are listed among wearables such as physical, chemical or optical devices. In particular, physical sensors remain a winning technology due to their durability and signal stability [8-12]. Physical flexible and stretchable sensors offer a wide range of applications and they can detect pressure, friction or torsion as well as body movements [13-19]. Moreover, these devices can be embedded in the tissue in different ways, providing appealing integrated solutions for the usage of smart garments [20-24]. Among different materials, conductive thermoplastic elastomers (CTPE) result very attractive as strain gauge sensors since they exhibit a high thermal and chemical stability, as well as a tunable conductivity [25]. Usually, CTPE can be produced adopting low cost manufacturing processes such as micro-

Manuscript accepted on 03/11/2022. Corresponding author: Francesco Maita.

Francesco Maita and Luca Maiolo are with the Institute for Microelectronics and Microsystems of the CNR (IMM-CNR), Rome, 00133, Italy (e-mail: francesco.maita@cnr.it; luca.maiolo@cnr.it).

Veronica Piccialli is with "Sapienza", Università di Roma, 00185 (e-mail: veronica.piccialli@uniroma1.it).

Flavia Pensa is with "Università degli studi di Roma Tor Vergata", Via Cracovia 50, 00133, Rome, Italy (e-mail: fpensa97@gmail.com)

Marco Scatto is with Dept. of Science and Technology of Bio and Nanomaterials, University of Ca' Foscari, Venice, 30172, Italy (e-mail: marco.scatto@unive.it, marco@marcoscatto.com).

Massimiliano Ruggeri is with STEMS-CNR, Via Canal Bianco 28, Ferrara, 44124, Italy (massimiliano.ruggeri@stems.cnr.it).

extrusion and injection molding, and they can be easily controlled by tuning the type of nanostructures embedded in the filler, thus obtaining variable resistances as sensors [26]. On the other hand, these materials often need long and time-consuming procedures to stabilize their response in time according to pre-strained procedures to reduce the drift of CTPE sensor. Indeed, even if these materials generally respond very quickly to a mechanical stimulus, they undergo to rearrangement of their internal nanostructures, producing a strong drift due to a relaxation of the elastic part of the sensor. In this sense, it should be considered the possibility to use CTPE materials that can exhibit minimal drift or even a stable response without the imposition of long pre-conditioning procedures. To achieve this result, we have to consider both the different type of nanostructures that can be used for manufacturing the material (e.g. spherical or asymmetrical carbon elements) and the modality in which the sensor should operate (pre-plastic, elastic etc.) [27]. In this work, we demonstrate the implementation of a nanostructured CTPE strain sensor, operating in a specific mode that permits to avoid pre-conditioning cycles and maintain a stable response in time for a range of strain up to 20%. The performance of the sensors is compared with a pre-strained device. Finally, to show the full potential of the device, sensor response is observed even on a smart wristband to detect specific gesture, thus opening the possibility to use these devices as key elements for biomedical applications.

II. Sensor Fabrication

CTPE sensor material has been provided in form of wires by Nadir srl. Both TPE pellets (the elastomeric matrix) and carbon-based powder (the conductive nanofiller) are fed through volumetric dispensers in the main hopper of a Lab Scale Co-rotating Twin Screw Extruder by Thermofisher. The kneading screw (d=12 mm) is structured in 8 zones with three interposed sections to produce high-uniformity blends. The temperature profile is set at 180 °C for the first zone and 200 °C for the other ones while the screw rotation speed is kept constant at 100 rpm to limit the variations in the density of the produced material. Through several trials a wire with 0.8 mm diameter and a nominal resistivity of 15 Ωcm has been produced (Fig.1).

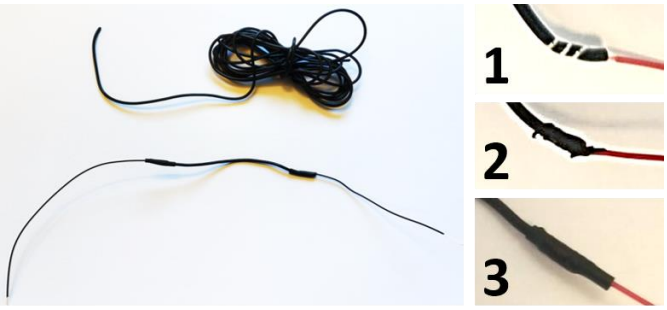

Fig. 1. On the left side, the spool of the extruded wire (above) and electrically connected sensor (below). On the right side, the process to form a reliable electrical and mechanical contact: 1) bare wire (red) is wrapped around 0.5cm of CTPE material; 2) mixture of carbon filled paste and glue is placed around the contact zone to improve contact resistance and act as mechanical bonder; 3) heat-shrinkable tube is inserted to further improve mechanical reliability.

This value of resistivity enables the production of sensors with a total resistance in the range of hundreds of kΩ, making easier integrating the devices with standard circuitry for many use cases. The material looks very stretchable and it withstands elongation in pre-strain mode up to 400 % without breaking down. After the extrusion, the sensing material was cut in wires 5.5 cm long. Durable connections have been made following the process shown in Fig.1: a bare wire has been wrapped around the material and fixed by using a blend of graphite powder with glue. Heat-shrink tubes have been embedded in the wire-to-polymer contact zone to increase the mechanical stability and to provide electrical insulation. The sensors have been tested as is, without any additional coverage, at room temperature.

III. Experimental

A. Material without pre-straining

To observe the behavior of the sensor in the different conditions a mechanical setup based on stepping motors has been used. In particular, a linear elongation has been superimposed to the device, controlling the sensor response by an ad hoc software compiled in LabView. Software sends command to a stepper motor by Contek (speed up to 2 mm/s) with a resolution in positioning down to 1µm and communicate with a Keythley 2440 for the resistance measurement. The software records the electrical resistance as a function of the elongation and it is able to perform cycling of type elongation-pause-relaxation-pause, allowing to measure characteristic curves such as Normalized resistance variation vs Strain (Fig.2), stress test over many cycles, analysis of the sensor response to constant strain and dynamic response to different strain speed (Fig.3a-b-c-d).

To limit the detrimental effect of long-term drift of the resistance rest value of the sensor, the devices have been annealed before the mechanical measurements with a soft-bake of 8 hours at 60 °C. This allows to reduce the content of water due to long term absorption of air humidity caused by the lack of an encapsulation layer and to obtain reproducible results from different sets of tests.

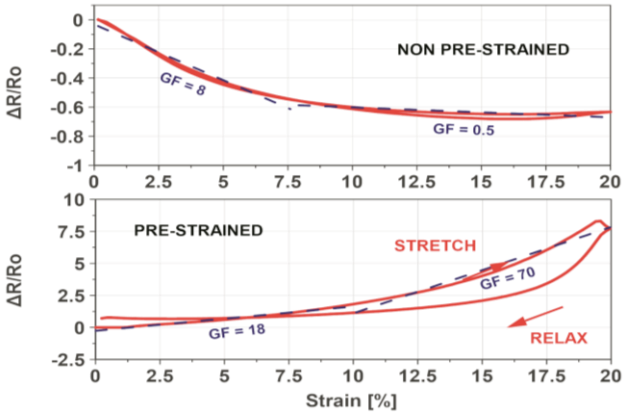

Fig. 2. Resistance variation vs. Strain in a single cycle for not-prestrained device (top) and for a pre-straining device with a treatment of 500 cycles at 250% (bottom). In blue (dashed line), both non pre-strained and pre-strained curve have been fitted as a combination of two lines to highlight the gauge factor in the different working regions.

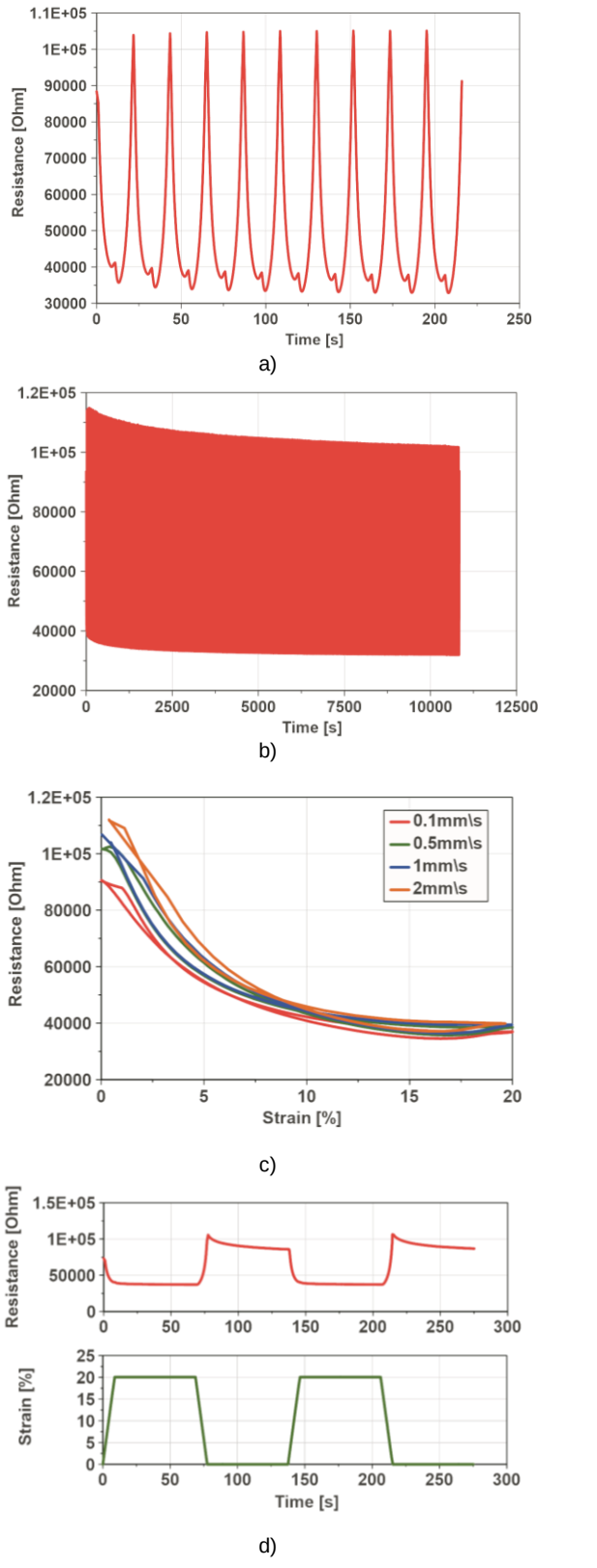

Fig. 3. (a) Measured resistance over 10 stress/relax cycles for a strain of 20% and a speed of 1 mm/sec for the sensor without pre-strain. (b) Sensor response for 500 stress/relax cycles at 20%, where 10% of drift in the resistance can be appreciated. (c) Response of S_{AE} to different stretching speeds. (d) Response of S_{AE} to static strain over a stretch/relax time of 60 s.

In these conditions, the sensor resistance at rest is in the range of 100 kΩ with a difference of less than 5% among the set of devices cut together, proving a very good uniformity of the extruded blend.

The plot of Fig.2 shows the behavior of the electrical resistance as a function of the strain with a linear speed of 1 mm/s. We tested two sensors using respectively the material as-extruded (S_{AE}) and pre-strained at 250% (S_{PS}). A very different behavior can be appreciated in this figure. In fact, not only the absolute values of R_0 and the dynamic range, but even the sign of the variation is different.

On one hand, S_{PS} increases its resistance vs the strain and has sensitivity about 8 times bigger respect to S_{AE} ($\Delta R/R_{0\text{-}PS}$ ~16 vs $\Delta R/R_{0\text{-}AE}$ ~ 2), but it exhibits higher hysteresis and a rest value an order of magnitude larger. On the other hand, S_{AE} decreases its resistance for increasing strain and the curve shows very low hysteresis comparing stretching and relaxing phase, resulting in a very stable curve.

In order to design a robust wearable application, we decided to prioritize stability over sensitivity and several tests were run to characterize the sensor behavior to short and long stresses (Fig.3a-b).

The plot of Fig.3a shows the behavior of the device-under-test (DUT) to ten consecutive cycles of stretching and relaxing. As it can be noticed, except for the first cycle where the initial value of the device is in the range of 90 kΩ, the device shows a very reproducible behavior during the following cycles (error on peak values <2%). The different value at t=0 of the plot has two causes: 1) the impossibility for the operator to put the sensor between the clamps of the test setup imposing zero mechanical stress; 2) elastomeric rearrangement due to the long preparation time. The local peak in the range of 40 kΩ that happens at the maximum strain point is well-known in literature for TPE based sensors and it is usually attributed to the time constants of elastomeric rearrangements happening at microscopic level [28,39].

Fig.3b displays a test run for 500 cycles keeping constant the measurement parameters. The plot shows a decrease of about 10% in the peak value at the end of the test, demonstrating a good stability of the device under stress conditions. Moreover, if ΔR and not absolute values are considered, the error goes down to 6-7%. While other types of strain gauge technologies can achieve better results in term of stability [34, 36], these values are in line with TPE/TPU based sensors [32] and are good enough to comply with the integrability of these devices in real applications (i.e. wearable electronics) since these changes can be managed easily with a proper circuit design.

The contribution of elastomeric time constants can be observed more clearly in Fig.3c, where S_{AE} is strained at different speeds. In fact, while the resistance at maximum strain is similar for all the speeds, the resistance changes visibly at rest position, because in this condition relaxation phenomena can happen more freely. This effect is more clearly observed in Fig. 3d. In this test the sensor is stretched up to 20% strain and left in static conditions for 60s. Then, it is relaxed down to 0% and left at rest for other 60s. It can be noticed how the value at max strain

is very stable while the value at 0% strain tends to decrease with a time constant in the order of tenths of seconds.
We calculated the performance of the devices in terms of the gauge factor (GF) as in Eq.1, fitting the data of Fig. 2 as a combination of two linear components, obtaining values of the GF up to 8 S_{AE} for and 70 for $S_{PS.}$

$$GF = \frac{\Delta R/R}{\Delta l/l} \quad \text{(Eq.1)}$$

These numbers are not particularly high compared to other works in literature where sensors with GF in the range of hundreds or thousands have been realized [29-36], but we designed these devices to optimize the overall performance of the sensor in terms of material cost, fabrication process cost and scalability, reproducibility, resistance value, circuit design, stability, strain range and GF, considering their integration on wearable applications more than maximizing the sensitivity of the sensor itself. In fact, even if it's possible to enhance greatly the gauge factor of the sensor pre-conditioning the strain gauge with many cycles of stretch-relax, this has two important side-effects: 1) it causes the material to have a mechanical residual stress that causes drift of resistivity and variability of the performance even over short time (see Fig.4) and 2) it increases dramatically the production time and costs.

B. Pre-strained material

We decided to compare the performances of the sensors without any mechanical treatment with the those that undergo a pre-strain.

At first, the wire has been stretched with increasing intensities to identify the pre-plastic regime, detected at about 400 % of the initial length. Then, 500 cycles have been imposed on the devices at 1mm/s in order the stabilize the polymeric blend. Finally, the elongated wire has been cut again in pieces of the same length of the unstrained ones. The result of the comparison is shown in Fig.2. The most remarkable effect of the pre-strain process is the inversion of the trend of the resistance as function of the elongation, from "negative strain effect" to "positive strain effect" (more details in the paragraph "C – Positive vs negative strain effect").
It has to be noted that the inversion of the resistance curve is not the only effect of the pre-strain. In fact, comparing the resistance value in the two cases, the pre-strained sensor has a resistance more than 1 order of magnitude higher than the non-pre-strained one. Such huge difference is due to the intrinsic non-linear response typical of this kind of elastomeric blends. In fact, such trend is noticeable in all the characteristic curves and is even more remarkable for higher strain, causing the device to work in resistance ranges as high as hundreds of MΩ to few GΩ.

This aspect needs two different considerations: from one hand, the pre-strained sensor gains in terms of GF. In fact, applying Eq.1, the gauge factor of pre-strained devices is about 70, considerably higher than non-pre-strained devices (8). From the other hand, designing circuits that works with very high resistances is difficult because of matching problems and noise.

Another important aspect about pre-conditioned devices is shown in Fig.4. Pre-strain tends to leave residual stress in the material. This causes variations in cycle-to-cycle sensor response that can be significative and, hence, detrimental to its circuit integration. Even if this effect can be drastically reduced tuning finely the pre-strain level and increasing the number of cycles, this causes the process to be even more time consuming and not very suitable for an industrial and scalable approach.

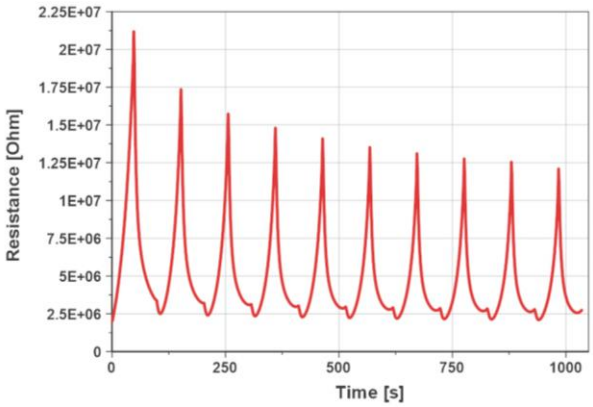

Fig. 4. Resistance variation of pre-strained sensors over consecutive cycles. A very large drift in the rest value is visible even for a short amount of cycles.

C. Positive vs negative strain effect

The sensing mechanism at the base of CTPE devices involve the formation of a percolation network between the conductive nano-particles and the elastomeric matrix. When strained, the device undergoes a volumetric change that affects the distance and the contact area among the particles and, macroscopically, the electrical resistance. The way this volumetric change happens and the way the particles rearrange in the device depends on many elements such as the filler size, shape and density, the shape of the device, the elastic constant, the relaxation time constants, etc. [37,38]. The precise phenomena are hard to investigate and are still object of study in the scientific community, but an in-depth explanation of the mechanics principles can be found in [39].
Based on the properties of the extruded material in terms of the nanofiller shape, density and distribution and on the experimental data collected it is possible to assume three different electrical configurations: in initial conditions (Fig.5a) the conductive nanoparticles (blue) are distributed in the polymeric matrix and the current path (black) is well established. For low levels of strain, the distance among the particles on wire axis increases while the one on the radius direction decreases. If the elastic response of the polymer is anisotropic along the two axis it can happen that the mechanic deformation has a bigger effect on the radius axis (See Fig.1b in [39]). This effect, together with a high concentration of conductive nanoparticles, makes possible a current path rearrangement that results, macroscopically, in a decrease of the resistance (Fig.5b). Necessarily, for high levels of strain, the distance of the particles along the current path increases, finally resulting in a resistance increase (Fig.5c).

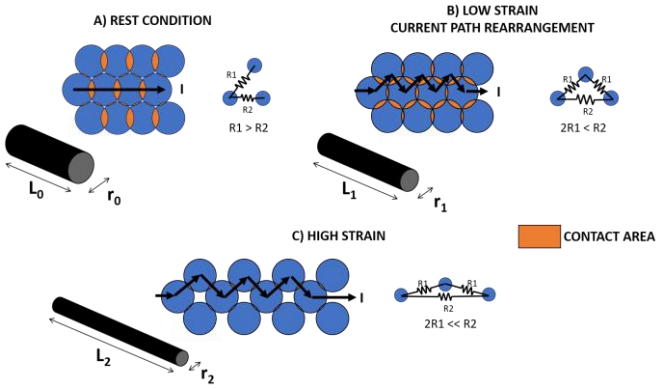

Fig. 5. Elastic rearrangement phases in the sensor material during applied strain in material with high conductive filler densities and anisotropic elastic behavior. Highlighted in orange, the contact area: a bigger contact area implies a lower resistance path among conductive particles.

IV. Smart Wristband Fabrication

To demonstrate the applicability of these kind of devices in real applications we designed and fabricated a smart cloth wristband prototype. In fact, such applications fit very well with all the discussed properties of these sensors in terms of size, shape, sensitivity, mechanical deformation range and electrical resistance range.

We designed a simple electronic board based on an Arduino Nano 33 IoT, that is used for both data acquisition (12-bit ADC) and transmission (Bluetooth/WiFi). The power is provided through a low-noise voltage regulator by a 500 mAh, 3.7 V Li-Po battery.

The acquisition chain is depicted in Fig.6a: the sensor is arranged in a voltage divider configuration where the constant resistor is set to approximately the same value of R_0 to maximize the dynamics. The generated signal is fed through a decoupling buffer, a low-pass filter ($f_{CUT\text{-}OFF}$ = 100 Hz) and a Programmable Gain Amplifier. The gain has been set to 8 for the scope of this work. Finally, the data are digitized through the ADC channels of the Arduino board and sent through BLE protocol to a custom Python software, that manages both storage and data analysis.

The electronic components have been attached to an elastic fabric using Velcro tape, even used for locking and unlocking the wristband (Fig.6b). The wires connecting the sensors have been inserted inside the band fabric and glued at the sensor sides to avoid that the wrist deformation occurring when the user is using the wristband, move the wire connections instead of stretching the sensor. In particular, 3 sensors fabricated using as-extruded material have been integrated on the internal side of the band, directly in touch with the skin (Fig.6).

The sensors have been distributed at a distance of 1.5 and 2.5 cm along the arm axis to cover a more extended area of the wrist.

The system is embedded with a 6-axis IMU (LSM6DS3): in this way the band is able to track fine movements of the wrist together with wider movements of the arm. On one hand, this provides a more valuable dataset. On the other hand, it allows to better evaluate the performance of the strain gauges through a comparison with or without IMU data.

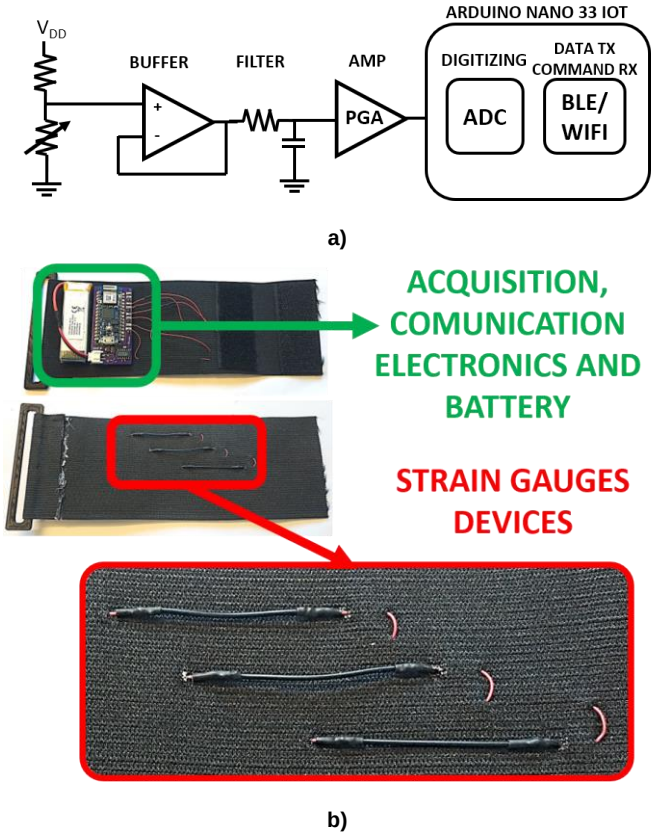

Fig. 6. a) Functional schema of the circuit used for sensor data acquisition; b) Picture of the smart wristband from top view and bottom view. On the bottom, the detail of the 3 strain gauge devices distributed at different lengths to detect the diverse movements of the wrist.

V. Discussion

To validate the use of the wristband, we built a dataset consisting of 101 repetitions for 14 different gestures, getting a dataset of 1414 examples. The selected gestures and typical experimental data can be seen in Fig.7a-b. Dataset has been built through 10 different acquisition sessions with 10 repetitions of each gesture performed for each session. At the end of each session the wristband has been removed and worn again. This procedure has been performed to ensure enough robustness in the processed results, being the device fabricated on elastic fabric and slight differences on how much the band is stretched and how it is positioned are unavoidable.

The tests have been conceived to build a classifier able to recognize the different hand gestures by the data registered by the wristband.

TABLE I
PERFORMANCE INDICATORS FOR GESTURE RECOGNITION

Index	Strain gauge only	Strain gauge + IMU
Accuracy	0.94326	0.99291
F1 Score	0.94871	0.99476

Accuracy and F1 Score for gesture recognition in wristband considering the contribute from strain gauges alone and with IMU data.

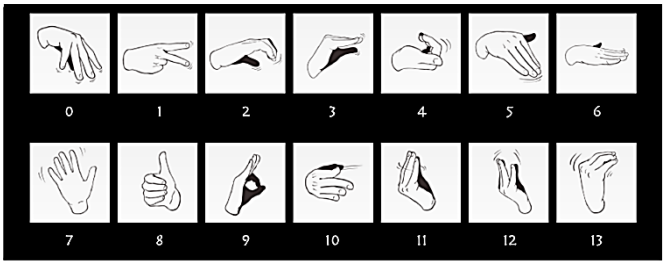

a)

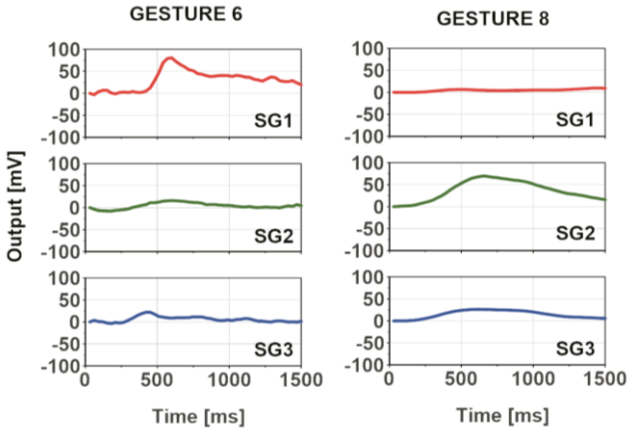

b)

Fig. 7. a) Set of gestures that have been used to train the convolutional neural network; b) normalized strain gauge data relative to one sample acquisition of gesture 6 (left) and 8 (right)

We split the dataset into training and test, to evaluate the performance of unseen data. As a classifier, we implemented a Convolutional Neural Network (CNN), following the recent literature, see for example [40], [42], [43] and [44]. The network architecture consists of 16 convolutional layers, followed by a deep dense neural network to perform the classification. The convolutional layers extract the features relevant to the input time series. The dense layers exploit the extracted features to classify the hand gestures. The choice of a convolutional neural network is due to its well-known ability to capture the temporal relationship in a time series (see [41]). The CNN network returns in output a probability for each hand gesture, given the sensors' time series in input. The gesture receiving the highest probability is the predicted gesture.

We built two different datasets: one containing only the time series relative to the as-fabricated strain gauge sensors, and the other containing the ones relative to all the sensors (strain gauges + IMU). For each sensor and each repetition of every hand gesture, we tested in cross validation different lengths for the time series, and the best values turned out to be 50. To train the network, we minimized the categorical cross-entropy loss, and employed the ADAM algorithm with learning rate 0.001, maximum number of epochs equal to 1000, and an early stopping patience set to 20. The network has impressive performance on the test set, especially when all the sensors, both strain gauges and IMU, are concatenated. To evaluate the model, we use the accuracy (the percentage of correctly predicted data) and the F1 score (harmonic mean of precision and recall). The two metrics are between 0 and 1, and a higher value implies better performance.

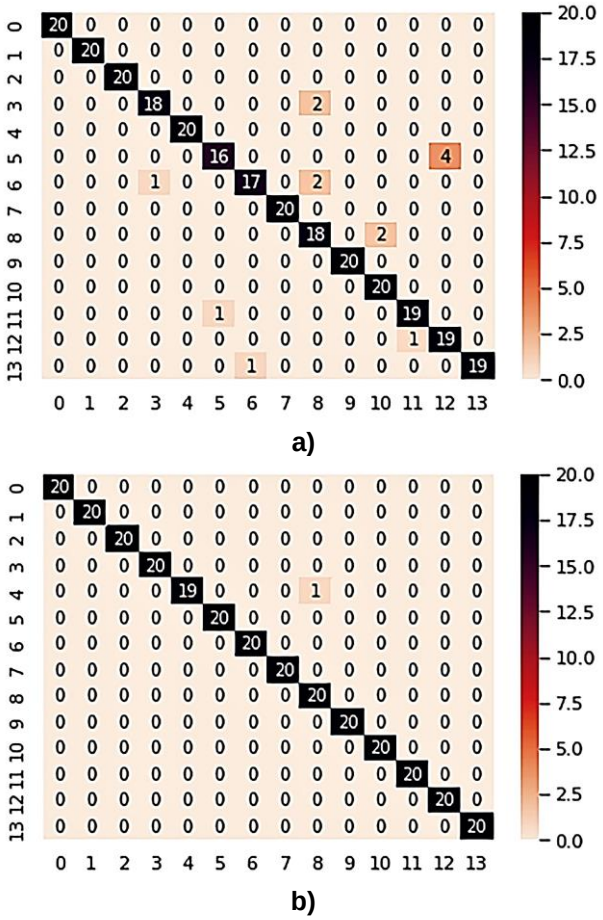

Fig. 8. Comparison between the confusion matrix for the gesture recognition when only strain gauge sensors are considered (a) and when all the sensors (strain gauge + IMU) are considered.

In Table 1 we report the two metrics on the test set, both when only strain gauge sensors are included, and when all the sensors are considered. Combining all the sensors leads to very high accuracy and F1 score, showing the effectiveness of the approach. To better appreciate the results, we report also the confusion matrix on the test set for the dataset containing only the strain gauge sensors and the one with all the sensors concatenated in figures Fig.8a and Fig.8b respectively.

As we can see, when only the strain gauge sensors are used, the method misclassifies 13 gestures out of 280, and the largest number of errors is when gesture 5 is executed, and it is confused with gesture 12. When all the sensors are concatenated, the method misclassifies only once gesture 4, interpreting it as gesture 8. The performance is impressive, considering also how similar some of the gestures are (see for example gestures 11, 12 and 13 that are very similar).

VI. Conclusions

In this work we fabricated and characterized CTPE based strain gauge sensors. The polymer blend has been optimized to produce sensors with an electrical resistance in the order of tenths of kOhm to be easily integrated in electronic circuits. We compared the performance of pre-conditioned and not pre-

conditioned devices, demonstrating how the latter, thanks to both its mechanical stability and shorter fabrication time can represent an ideal solution to realize wearable electronics applications where small variations (5÷20%) need to be detected with precision. Finally, we validated our approach designing and fabricating a cloth-based smart wristband implementing such sensors and commercial electronics for data acquisition and transmission, demonstrating our capability to distinguish up to 14 different gestures with a state-of-art accuracy of 94% using only strain gauges data and 99% considering IMU sensors. These results are particularly relevant when compared to similar works in literature considering that we used only 3 sensors without a dedicated study to the optimization of the size, the number and the position of the sensor themselves. In fact, even if F-Score and accuracies can be on comparable levels, these results often come at the cost of adopting invasive solutions [45-47], a large number of sensors [45] or recognizing a very limited set of gestures [48-50]. These considerations let us estimate that the obtained results just scratch the real potential of an appealing technology for studies and applications related to human body movement analysis such as gesture recognition, gait analysis, motion tracking, etc.

REFERENCES

[1] M. Stoppa and A. Chiolerio, “Wearable Electronics and Smart Textiles: A Critical Review”, Sensors, *14*(7), 11957-11992 (2014)

[2] Heo, J. S., Eom, J., Kim, Y.-H., Park, S. K, “Recent Progress of Textile-Based Wearable Electronics: A Comprehensive Review of Materials, Devices, and Applications”, Small 2018, 14, 1703034, (2018)

[3] N. A. Choudhry, L. Arnold, A. Rasheed, I. A. Khan and L. Wang,., “Textronics—A Review of Textile-Based Wearable Electronics”, Adv. Eng. Mater., 23: 2100469, (2021)

[4] K. Xu, Y. Lu and K. Takei, Multifunctional Skin-Inspired Flexible Sensor Systems for Wearable Electronics, Adv. Mater. Technol., 4, 1800628 (2019)

[5] Y. W. Chong, W. Ismail, K. Ko and C. Y. Lee, "Energy Harvesting for Wearable Devices: A Review," in IEEE Sensors Journal, vol. 19, no. 20, pp. 9047-9062, (2019)

[6] Z. Duan, Y. Jiang, S. Wang, Z.Yuan, Q. Zhao, G. Xie, X. Du and H. Tai, “Inspiration from Daily Goods: A Low-Cost, Facilely Fabricated, and Environment-Friendly Strain Sensor Based on Common Carbon Ink and Elastic Core-Spun Yarn”, ACS Sust. Chem & Eng., 7, 17474-17481, (2019)

[7] Y. Zheng, R. Yin, Y. Zhao, H. Liu, D. Zhang, X. Shi, B. Zhang, C. Liu and C. Shen, “Conductive MXene/cotton fabric based pressure sensor with both high sensitivity and wide sensing range for human motion detection and E-skin”, Chem. Eng. Journal, 420, 127729, (2021)

[8] Y. Jiao, C. W. Young, S. Yang, S. Oren, H. Ceylan, S. Kim, K. Gopalakrishnan, P. C. Taylor and L. Dong, "Wearable Graphene Sensors with Microfluidic Liquid Metal Wiring for Structural Health Monitoring and Human Body Motion Sensing," in IEEE Sensors Journal, vol. 16, no. 22, pp. 7870-7875, Nov.15, (2016)

[9] T.Q. Trung, S. Ramasundaram, B. U. Hwang, and N. E. Lee, “An All-Elastomeric Transparent and Stretchable Temperature Sensor for Body-Attachable Wearable Electronics”, Adv. Mater., 28: 502-509, (2016)

[10] A. Pecora, L. Maiolo, A. Minotti, R. De Francesco, E. De Francesco, F. Leccese, M. Cagnetti and A. Ferrone, "Strain gauge sensors based on thermoplastic nanocomposite for monitoring inflatable structures," 2014 IEEE Metrology for Aerospace (MetroAeroSpace), Benevento, pp. 84-88 (2014)

[11] A. Ferrone, X. Jiang, L. Maiolo, A. Pecora, L. Colace, C. Menon, “A fabric-based wearable band for hand gesture recognition based on filament strain sensors: A preliminary investigation”, 2016 IEEE Healthcare Innovation Point-Of-Care Technologies Conference (HI-POCT), pp. 113-116, (2016)

[12] L. Maiolo, F. Maita, A. Pecora, A. Minotti, G. Fortunato, E. Smecca, A. Alberti, “A comparison among low temperature piezoelectric flexible sensors based on Polysilicon TFTs for Advanced Tactile sensing on plastic”, Journal of Dis. Tech., Vol.12, I3, pp.209-213, (2016)

[13] S. Gong, W. Schwalb, Y. Wang, , “A wearable and highly sensitive pressure sensor with ultrathin gold nanowires”, Nat Commun 5, 3132 (2014)

[14] A. Ferrone, F. Maita, L. Maiolo, A. Arquilla, A. Castiello, A. Pecora, X. Jiang, C. Menon and L. Colace, ″Wearable band for hand gesture recognition based on strain sensors″, 2016 6th IEEE International Conference on Biomedical Robotics and Biomechatronics (BioRob), Singapore, pp. 1319-1322 (2016)

[15] A. Chortos and Z. Bao, “Skin-inspired electronic devices”, Materials Today, Volume 17, Issue 7, pp 321-331, (2014)

[16] H. Liu, H. Xiang, Y. Wang, Z. Li, L. Qian, P. Li, Y. Ma, H. Zhou and W. Huang, “A flexible multimodal sensor that detects strain, humidity, temperature, and pressure with carbon black and reduced graphene oxide hierarchical composite on Paper”, ACS Appl. Mater. Interfaces, 11, 40613-40619, (2019)

[17] Y. He, D. Wu, M. Zhou, Y. Zheng, T. Wang, C. Lu, L. Zhang, H. Liu and C. Liu, “Wearable strain sensors based on a porous polydimethylsiloxane hybrid with Carbon nanotubes and Graphene”, ACS Appl. Mater. Interfaces, 13, 15572-15583, (2021)

[18] S.Q. Zhao, P.X. Zheng, H.L. Cong and A.L. Wan, “Facile fabrication of flexible strain sensors with AgNOs-decorated CNTs based on nylon/PU fabrics through polydopamine templates”, Appl. Surf. Sci. 558, 149931, (2021)

[19] J. Shu, R. Yang, Y. Chang, X. Guo and X. Yang, “A flexible metal thin film strain sensor with micro/nano structure for large deformation and high sensitivity strain measurement”, Jour. Of Alloys and Compounds, Vol. 879, 160466, (2021)

[20] S. Zhang, A. Chhetry, A. Zahed, S. Sharma, C. Park, S. Yoon and J.Y. Park, “On-skin ultrathin and stretchable multifunctional sensor for smart healthcare wearables”, npj Flexible Electronics 6:11, (2022)

[21] D. De Rossi, F. Carpi, F. Lorussi, R. Paradiso, E. P. Scilingo and A. Tognetti, “Electroactive fabrics and wearable man-machine interfaces”. In X. Tao, editor, Wearable electronics and photonics. 298 Flexible wearable electronics for monitoring application Woodhead Publishing in Textiles, Ch.4, pp. 59–80, (2005)

[22] O. Atalay, W. R. Kennon and E. Demirok, “Weft-Knitted Strain Sensor for Monitoring Respiratory Rate and Its Electro-Mechanical Modeling” IEEE Sensors Journal, vol. 15, no. 1, pp. 110-122, (2015)

[23] Y.A. Samad, K. Komatsu, D. Yamashita, Y. Li, L. Zheng, S. M. Alhassan, Y. Nakano, K. Liao, “From sewing thread to sensor: Nylon fiber strain and pressure sensors”, Sens. And Actuators B 240, pp. 1083-1090, (2017)

[24] L. Lu, Y. Zhou, J. Pan, T. Chen, Y. Hu, G. Zheng, K. Dai, C. Liu, C. Shen, X. Sun, and H. Peng, “Design of helically double-leveled gaps for stretchable fiber strain sensor with Ultralow detection Limit, Broad Sensing Range and High Repeatability”, ACS Appl. Mater. Interfaces, 11, pp. 4345-4352, (2019)

[25] Z. Liu, T. Zhu, J. Wang, Z. Zheng, Y. Li, J. Li, Y. Lai, “Functionalized Fiber-Based strain sensors: Pathway to Next-Generation wearable electronics”, Nano-Micro Lett., 14:61, (2022)

[26] H. Liu, Y. Li, K. Dai, G. Zheng, C. Liu, C. Shen, X. Yan, J. Guo and Z. Guo, “Electrically conductive thermoplastic elastomer nanocomposites at ultralow graphene loading levels for strain sensor applications”, J. Mater. Chem. C,4, pp. 157-166, (2016)

[27] S. Coiai, E. Passaglia, A. Pucci and G. Ruggeri, “Nanocomposites Based on Thermoplastic Polymers and Functional Nanofiller for Sensor Applications”, Materials, 8(6), pp. 3377-3427, (2015)

[28] L. Flandin, A. Hiltner and E. Baer, “Interrelationship Between Electrical and Mechanical Properties of a Carbon Black-Filled Ethylene–Octene Elastomer”, Polymer 42(2):827-838, (2001)

[29] X. Liao, Z. Zhang, Z. Kang, F. Gao, Q. Liao and Y. Zhang, “Ultrasensitive and stretchable resistive strain sensors designed for wearable electronics”, Mater. Horiz., 4, 502, (2017)

[30] S. Jang, J. Kim, D. W. Kim, J. W. Kim, S. Chun, H. J. Lee, G. Yi and C. Pang, “Carbon-Based, Ultraelastic, Hierarchically Coated Fiber Strain Sensors with Crack-Controllable Beads”, ACS Appl. Mater. Interfaces,11, pp. 15079−15087, (2019)

[31] X. Liao, W. Wang, L. Wang, K. Tang and Y. Zheng, “Controllably Enhancing Stretchability of Highly Sensitive Fiber-Based Strain Sensors for Intelligent Monitoring”, ACS Appl. Mater. Interfaces, 11, pp. 2431−2440, (2019)

[32] Y. Zhao, M. Ren, Y. Shang, J. Li, S. Wang, W. Zhai, G. Zheng, K. Dai, C. Liu and C. Shen, “Ultra-sensitive and durable strain sensor with

sandwich structure and excellent anti-interference ability for wearable electronic skins", Comp. Sci. and Tech. 200, 108448, (2020)
[33] H. R. Na, H. J. Lee, J. H. Jeon, HJ. Kim, SK. Jerng, S. B. Roy, SH. Chun, S. Lee, Y. J. Yun, "Vertical graphene on flexible substrate, overcoming limits of crack-based resistive strain sensors", npj Flexible Electronics 6:2, (2022)
[34] Y. Lin, Q. Yin, L. Ding, G. Yuan, H. Jia and J. Wang, "Ultra-sensitive flexible strain sensors based on hybrid conductive networks for monitoring human activities", S&A: A Physical 342, 113627, (2022)
[35] X. Liao, W. Song, X. Zhang, H. Jin, S. Liu, Y. Wang, A. V. Thean and Y. Zheng, "An Artificial Peripheral Neural System Based on Highly Stretchable and Integrated Multifunctional Sensors", Adv. Func. Mat. n31(24),2101107, (2021)
[36] Q. Huang, Y. Jiang, Z. Duan, Z. Yuan, B. Liu, Q. Zhao, Y. Zhang, Y. Sun, P. Sun and H. Tai, "Facilely constructed randomly distributed surface microstructure for flexible strain sensor with high sensitivity and low detection limit", J. of Phys. D: Appl. Phys. 54 284003, (2021)
[37] L. Duan, S. Fu, H. Deng, Q. Zhang, K. Wang, F. Chen and Q. Fu, "The resistivity–strain behavior of conductive polymer composites: stability and sensitivity", J. Mater. Chem. A, 2, 17085, (2014)
[38] J. Lu, X. Chen, W. Lu and G. Chen, "The piezoresistive behaviors of polyethylene/foliated graphite nanocomposites", Eur. Polymer J. 42, pp. 1015-1021, (2006)
[39] S. Kim, S. Choi, E. Oh, J. Byun, H. Kim, B. Lee, S. Lee and Y. Hong, "Revisit to three-dimensional percolation theory: Accurate analysis for highly stretchable conductive composite materials", Sci. Rep. 6, 34632 (2016)
[40] G. Devineau, F. Moutarde, W. Xi and J. Yang, "Deep Learning for Hand Gesture Recognition on Skeletal Data," 2018 13th IEEE International Conference on Automatic Face & Gesture Recognition (FG 2018), pp. 106-113, (2018)
[41] H. I. Fawaz, G. Forestier, J. Weber, L. Idoumghar and P-A. Muller, "Deep learning for time series classification: a review". Data Min Knowl Disc 33, pp. 917–963, (2019)
[42] W. Jiang, X. Ye, R. Chen, F. Su, M. Lin, Y. Ma, Y. Zhu and S. Huang, "Wearable on-device deep learning system for hand gesture recognition based on FPGA accelerator", Mathematical Biosciences and Engineering, 18(1), 132-153, (2021)
[43] X. Song, X. Liu, Y. Peng, Z. Xu, W. Liu, K. Pang & J. Meng, "A graphene-coated sild-spandex fabric strain sensor for human movement monitoring and recognition", Nanotechnology, 32(21), 215501 (2021)
[44] S. Jiang, P. Kang, X. Song, B.P.L. Lo and P.B. Shull, "Emerging wearable interfaces and algorithms for hand gesture recognition: A Survey", IEEE Reviews in Biomedical Engineering, Vol.15, pp.85-102, (2022)
[45] A. Moin, A. Zhou, A. Rahimi, A. Menon, S. Benatti, G. Alexandrov, S. Tamakloe, J. Ting, N. Yamamoto, Y. Khan, F. Burghardt, L. Benini, "A wearable biosensing system with in-sensor adaptive machine learning for hand gesture recognition", Nature Electronics, Vol.4, I.1, pp. 54-63, (2021)
[46] W. K. Wong, H. J. Filibert, B. T. T. Khoo, "Multi-features capacitive hand gesture recognition sensor: a machine learning approach", IEEE Sensors Journal, Vol.21, n.6, (2021)
[47] R. Ramalingame, A. Bouhamed, D. Rajendran, R. da Veiga Torres, Z. Hu and O. Kanoun, "Highly sensitive polymer/multiwalled carbon nanotubes based pressure and strain sensors for roboti applications", Studies in Sys., Dec. and Cont. 270, pp.371-382 (2020)
[48] H. Zhao, S. Wang, G. Zhou and D. Zhang, "Ultigesture: A Wristband-based platform for continuous gesture control in healthcare", Smart Health 11, pp.45-65, (2019)
[49] C. Shen, Y. Chen, G. Yang and X. Guan, "Toward Hand-dominated activity recognition systems with wristband-interaction behavior analysis", IEEE Trans. On Sys., Man, and Cyber.: Sys, Vol.50, n.7 (2020)
[50] Q. Gao, S. Jiang and P. B. Shull, "Simultaneous Hand gesture classification and finger estimation via a novel dual-output deep learning model", Sensors, 20, 2972, (2020)